

24 Abstract

25 The 2014–2017 global coral bleaching event caused widespread coral mortality; however, its
26 impact on the capacity for coral reefs to maintain calcium carbonate structures remained to be
27 determined. Here, we quantified remotely sensed maximum heat stress during the 2014-2017
28 bleaching event, census-based net carbonate budgets from benthic imagery and fish survey data,
29 and net calcification from salinity normalized seawater total alkalinity anomalies collected from
30 2017-2019 for 56 Pacific coral reef sites (Mariana Islands, Northwestern Hawaiian Islands,
31 Pacific Remote Island Areas, and American Samoa). We incorporated the census-based and
32 chemistry-based metrics to determine a calcification vulnerability index for each site to maintain
33 calcium carbonate balance to provide accessible information to managers and policy makers.
34 Most coral reef sites likely experienced ecologically severe (79%,n=44) or significant (9%,n=7)
35 heat stress during the 2014-2017 coral bleaching event. Census-based net carbonate budgets
36 (mean±95%=2.1±0.6 kg CaCO₃ m⁻² yr⁻¹) were positive for 77% of sites (n=43), neutral for 16%
37 of sites (n=9), and negative for 7% of sites (n=4). Chemistry-based net calcification
38 (mean±95%=22±10 μmol kg⁻¹) was positive for 84% of sites (n=47), neutral for 11% of sites
39 (n=6), and negative for 5% of sites (n=3). The calcification vulnerability index suggested the
40 Pacific Ocean reef sites surveyed were of minimal (68%,n=38) to moderate (32%,n=18) concern
41 for maintaining calcium carbonate balance following the bleaching event. This suggests that
42 many reefs maintained positive calcium carbonate balance, but that a large number of reefs may
43 be approaching a potential threshold for maintaining their calcium carbonate balance under the
44 climate crisis.

45

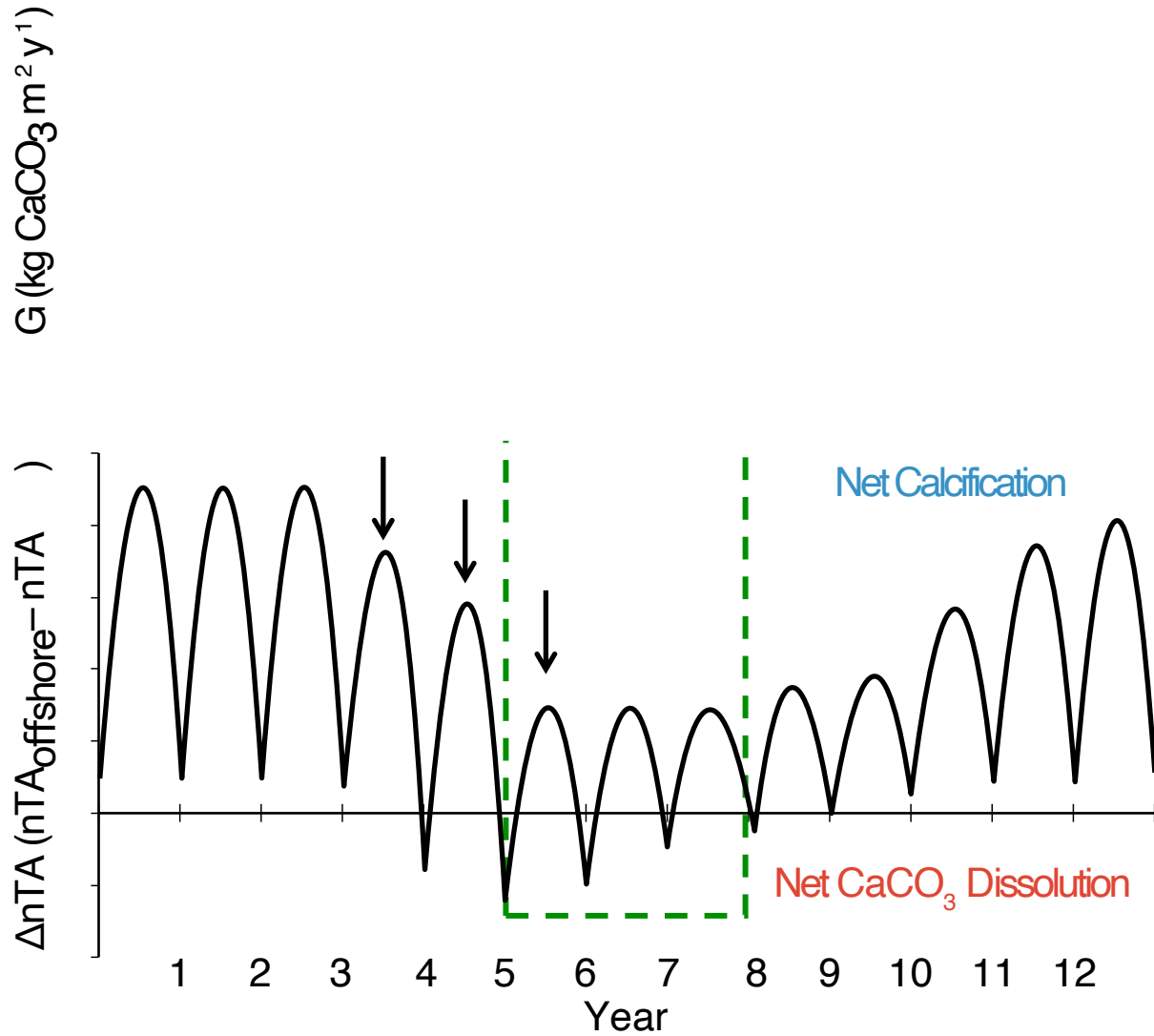
46 Introduction

47 Scleractinian corals are the primary reef-builders of the coral reef structures that sustain
48 ecosystem services ranging from shoreline protection, fisheries provisioning, cultural
49 significance, and tourism revenue for billions of people worldwide (Kleypas et al. 2001; Perry
50 and Alvarez-Filip 2019; Woodhead et al. 2019). However, global coral cover has declined
51 precipitously in recent decades under local and global environmental change (Gardner et al.
52 2003; Bruno and Selig 2007; De'ath et al. 2012) with the third global coral bleaching event from
53 2014-2017 further jeopardizing coral dominated reef states and associated maintenance of coral
54 reef structures (Eakin et al. 2019). Quantifying these changes in coral reef structures and their
55 associated geo-ecological functions represents a challenging task, but is essential to be able to
56 predict future changes to the ecosystem services coral reefs provide to the people that depend on
57 them (Perry and Alvarez-Filip 2019).

58 Quantifying changes in coral reef geo-ecological functions can be accomplished through
59 measuring the net accumulation of calcium carbonate (CaCO_3), but direct measurements of
60 changes in coral reef bathymetry or accretion rates from sediment cores typically require
61 multiple years to detect changes (Aronson and Precht 2001; Yates et al. 2017; Lange et al.
62 2020a). Census-based net carbonate budgets and chemistry-based net coral reef calcification
63 have been widely used to provide insights into the maintenance of coral reef structures under
64 environmental change (e.g., see discussion in (Courtney and Andersson 2019; Lange et al.
65 2020a; Browne et al. 2021) and references therein). Census-based methods sum annual CaCO_3
66 production and erosion rates of different functional groups to estimate net carbonate budgets
67 from ecological surveys, but are limited by survey biases (i.e., what the observer can see) and
68 typically rely on literature derived annualized rates (Chave et al. 1972; Perry et al. 2018b; Lange
69 et al. 2020a). Chemistry-based methods utilize changes in seawater total alkalinity (TA) to

70 provide temporal snapshots of net coral reef calcification (i.e., TA changes by a factor of two for
71 every mole of CaCO_3 precipitated or dissolved (Broecker and Takahashi 1966; Smith and Key
72 1975; Chisholm and Gattuso 1991)), but difficulties in constraining seawater hydrodynamics can
73 generate significant uncertainties (Venti et al. 2012; Lowe and Falter 2015; Courtney and
74 Andersson 2019). As a result, census-based net carbonate budgets (i.e., carbonate production –
75 bioerosion) and chemistry-based net calcification (i.e., calcification – CaCO_3 dissolution) are
76 inherently quantifying slightly different processes to provide independent snapshots of the
77 capacity for coral reefs to produce and maintain CaCO_3 structures. These methods quantify
78 processes on different spatial scales with census-based budgets typically quantifying net
79 carbonate production at the spatial scale of transects (i.e., tens of meters squared) and ecosystem-
80 scale chemistry-based metrics typically integrating net calcification of the hydrochemical
81 footprint modified by the benthos (i.e., hundreds to thousands of meters squared) (Courtney et al.
82 2016) (but see also tens of meters squared footprints for chemistry-based eddy covariance
83 methods (Berg et al. 2007)). Furthermore, depending on the frequency of observations, the two
84 methods reflect the net sum of processes on different timescales, i.e., census-based observations
85 typically reflect processes on annual timescales whereas individual chemistry-based observations
86 reflect the sum of processes occurring over hours to days depending on reef seawater residence
87 time (Figure 1). Both methods are generally time intensive, require a great deal of careful
88 consideration, and are typically associated with a range of uncertainties (Courtney et al. 2016;
89 Courtney and Andersson 2019; Lange et al. 2020a). These characteristics effectively limit each
90 method's power and capacity to quantify global-scale changes in coral reef geo-ecological
91 functions to ongoing ocean warming, acidification, and deoxygenation over a broad spectrum of
92 spatial and temporal scales.

Perturbations



93

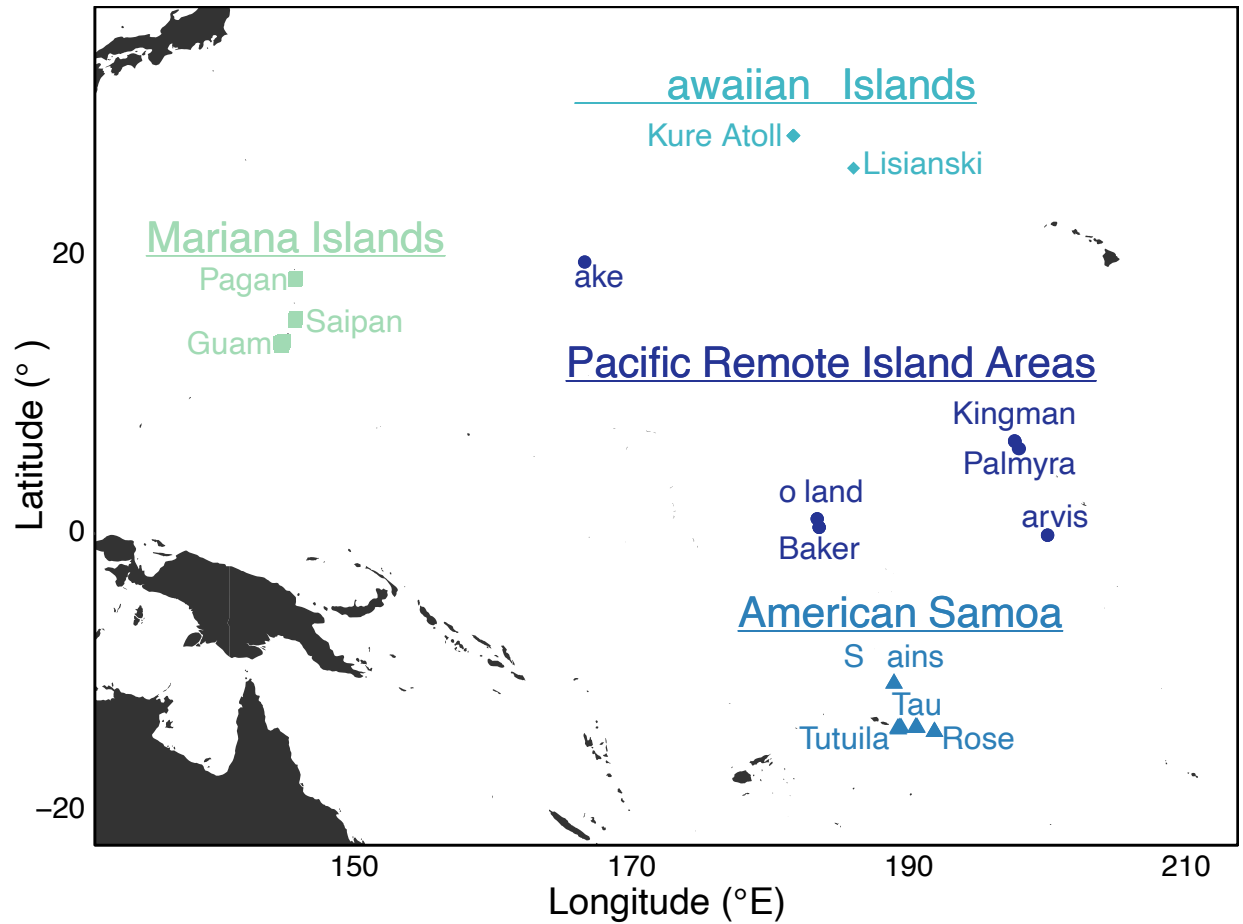
94 **Figure 1.** Conceptual figure showing hypothesized trends in census-based carbonate budget (G; top panel) and
95 chemistry-based net community calcification based on salinity normalized alkalinity anomalies (ΔnTA ; bottom
96 panel) for a coral reef exposed to multiannual perturbations (black arrows) over a 12-year period. The census-based
97 and chemistry-based data are based on annual and monthly observations, respectively. Note that individual
98 measurements over a limited observation period represent the net sum of processes occurring annually (census-
99 based) to over hours or days (chemistry-based), and thus, may not track each other and could even appear
100 contradicting without a complete temporal perspective. Regardless, these observations serve as important metrics in

101 the context of future global environmental change and observations, and especially if the measurements encompass
102 multiple reefs over a large spatial area. The hypothesized trends in the figure were adopted from observations
103 presented in (Yeakel et al. 2015; Courtney et al. 2018, 2020).

104

105 To address this limitation, we combined simplified assessments of census-based
106 carbonate budgets from benthic imagery and fish survey data and chemistry-based net
107 calcification from the difference between coral reef seawater TA and offshore seawater TA.
108 While each of these simplified metrics is associated with uncertainty, leveraging two
109 independent approaches increases confidence in assessing the maintenance of coral reef CaCO_3
110 structures, and also offers insight to chronic vs. acute concerns of the CaCO_3 balance across
111 varying spatial scales (Courtney et al. 2016; Courtney and Andersson 2019; Lange et al. 2020a).
112 We therefore applied these methods to pre-existing monitoring data from 56 coral reef sites
113 across the Mariana Islands, Northwestern Hawaiian Islands, Pacific Remote Island Areas, and
114 American Samoa to assess the following questions: (1) What is the capacity for coral reefs to
115 maintain their CaCO_3 structures following the 2014-2017 coral bleaching event based on the
116 census-based and chemistry-based approaches? (2) Does maximum heat stress experienced
117 during the 2014-2017 coral bleaching event or the commonly used metric of coral cover predict
118 our simplified carbonate budget and net calcification estimates? In addition to addressing these
119 questions, this synthesis provides critical baseline data and simplified, categorical assessments of
120 coral reef capacity to maintain CaCO_3 structures for managers and policymakers as part of
121 ongoing monitoring and conservation efforts.

122



123

124 **Figure 2.** Map of coral reef sites across the Mariana Islands, Northwestern Hawaiian Islands, Pacific Remote Island
 125 Areas, and American Samoa that were surveyed as part of the NOAA National Coral Reef Monitoring Program.

126

127 **Methods**

128 *Survey locations*

129 We leveraged coral reef benthic community composition, fish community composition,
 130 and carbonate chemistry data collected from designated coral reef climate monitoring sites
 131 (n=56) across the Pacific Ocean between 2017 and 2019 as part of the National Oceanic and
 132 Atmospheric Administration’s (NOAA) Pacific National Coral Reef Monitoring Program.

133 Surveyed reef locations included forereef sites at ~15 m depth in the Mariana Islands (16 sites

134 around Guam, Pagan, and Saipan in 2017), Northwestern Hawaiian Islands (6 sites around Kure
135 and Lisianski in 2019), Pacific Remote Island Areas (2 sites around Wake in 2017 and 18 sites
136 around Baker, Howland, Jarvis, Kingman, and Palmyra in 2018), and American Samoa (14 sites
137 around Rose, Swains, Tau, and Tutuila in 2018) (Figure 2).

138 *Census-based net carbonate budgets*

139 We used a simplified version of the census-based *ReefBudget* methodology (Perry et al.
140 2018b) to retroactively estimate carbonate production from benthic imagery data. At each site,
141 images were taken with a Canon G9x one meter off the substrate, every meter along each side of
142 a 15 m “L” shaped transect for a total of 30 images per site (see (Pacific Islands Fisheries
143 Science Center 2021) for further details on data collection). Ten random points in each image
144 were then annotated using the *CoralNet* image annotation software for a total of 300 annotations
145 per site (Beijbom et al. 2015). Corals were identified to genus or a combination of genus and
146 growth form for select genera (*Acropora*, *Montipora*, *Pavona* and *Porites*), macroalgae to genus,
147 and other benthic features to functional group or higher-level taxonomic grouping (e.g., ‘crustose
148 coralline algae’, ‘sand’, ‘sponge’, ‘turf algae’) using the NOAA CRED label set (n=95 labels) in
149 *CoralNet* (Lozada-Misa et al. 2017). Points were pooled across the transect tape to determine the
150 percent composition of each benthic feature at each site (Pacific Islands Fisheries Science Center
151 2021). The percent cover of each label was then multiplied by the area normalized Indo-Pacific
152 calcification rates with endolithic bioerosion for each benthic feature by (Courtney et al. 2021a)
153 and summed to calculate gross carbonate production and endolithic bioerosion for each site
154 (Perry et al. 2018b). These rates adapt the *ReefBudget* Indo-Pacific Carbonate Production v1.2
155 datasheet (Perry et al. 2018b) for use with *CoralNet* imagery by accounting for median colony
156 size, rugosity, colony morphology, linear extension, and skeletal density for all of the “NOAA

157 CRED” *CoralNet* identification labels *ReefBudget* methodologies (see (Courtney et al. 2021a)
158 for further details). While the uncertainty ranges in the rates from (Courtney et al. 2021a) used in
159 this study account for some degree of variability in rates across the Pacific Ocean, the use of
160 constant rates (\pm uncertainties) between sites does not account for any potential systematic
161 differences in rates between sites, which is a common limitation of census-based carbonate
162 budgets.

163 In the absence of co-located benthic survey and fisheries data, we used coral reef fish
164 survey data collected from stratified random sites around each of the islands (Pacific Islands
165 Fisheries Science Center 2017a; b; c, 2019a; b) to quantify gross parrotfish bioerosion (Perry et
166 al. 2018b). In each survey, two divers quantify the fish communities in paired 15 m diameter
167 cylinders using the stationary point count (SPC) method, identifying, counting, and estimating
168 the total length of fishes (see (Ayotte et al. 2011) for further details on data collection). We used
169 the data collected at mid-depth sites (>6-19 m) around islands in survey years that correspond
170 with the climate monitoring sites. However, matching fish community data was missing for the
171 2019 Northwestern Hawaiian Islands surveys so we used fish community data from 2017 and
172 therefore must make the assumption that parrotfish bioerosion rates determined from the 2017
173 data were similar to 2019 when the other benthic community composition and carbonate
174 chemistry data were collected.

175 Parrotfish bioerosion was estimated from the survey data as per the following allometric
176 relationship between body size and bioerosion rate from (Lange et al. 2020b): Bioerosion (kg
177 $\text{CaCO}_3 \text{ ind}^{-1} \text{ y}^{-1}$) = $a \times \text{TL}^b$. Constants a and b were empirically derived from linear regressions
178 between the log of the mid-point of total length (TL) in cm for each size bin and the log of the
179 corresponding bioerosion rate (kg $\text{CaCO}_3 \text{ ind}^{-1} \text{ y}^{-1}$) for initial and terminal phase fish for each

180 species from the *ReefBudget* Indo-Pacific Parrotfish erosion rates v1.3 data sheet (Perry et al.
181 2018b). We used the fixed bioerosion rate for *Bolbometopon muricatum* following (Perry et al.
182 2018b) and substituted mean genus-level bioerosion rates for taxon lacking species-level data.
183 While previous studies have documented differences between initial and terminal phase
184 bioerosion rates (Lange et al. 2020a), this information was lacking in the fish surveys so *a* and *b*
185 were therefore estimated for all parrotfish regardless of phase in this study. The resulting
186 species-specific bioerosion rates for each size bin and the resulting *a* and *b* constants used to
187 quantify parrotfish bioerosion rates from observed total length in this study are summarized in
188 Table S1. Individual parrotfish bioerosion per m² (survey area = πr^2 , where $r = 7.5$ m radius of a
189 cylinder) was summed in each replicate and then averaged between paired cylinders at each
190 survey site. Estimates were averaged across sites within a given stratum (island, reef zone, and
191 depth bin [all mid-depth]) and then pooled up to the scale of individual islands by weighting
192 strata by their proportional area within each island in accordance with the stratified survey design
193 (Heenan et al. 2017) to quantify mean (\pm SE) parrotfish bioerosion rates for each island.

194 Sea urchins were not directly quantified in the survey data, but the reef-fish surveys
195 qualitatively assessed relative abundance of sea urchins at each site and listed them as rare in
196 74.8% to 99.8% across the respective regions in this study (Pacific Islands Fisheries Science
197 Center 2017a; b; c, 2019a; b). Given the lack of robust sea urchin test size and density data
198 necessary to estimate sea urchin bioerosion following established methods (Perry et al. 2018b)
199 and their rare abundance at the majority of sites, we have omitted sea urchin bioerosion from this
200 study and therefore implicitly assume that they are not major sources of bioerosion across our
201 study sites.

202 Net carbonate budgets ($\text{kg CaCO}_3 \text{ m}^{-2} \text{ y}^{-1}$) were thus calculated as carbonate production
203 minus endolithic bioerosion and parrotfish bioerosion \times 50% reincorporation rate for each site
204 following (Perry et al. 2018a). While mechanical bioerosion by parrotfish is represented as a net
205 loss of CaCO_3 following *ReefBudget* methods (Perry et al. 2018b), there is limited data
206 quantifying the proportion of mechanically bioeroded CaCO_3 that is ultimately exported from the
207 reef environment (Browne et al. 2021). Here we have assumed that 50% of mechanical parrotfish
208 bioerosion was reincorporated back into the reef matrix with the remaining 50% exported from
209 the reef following (Hubbard et al. 1990; Perry et al. 2018a). We conservatively calculated the
210 lower bound of the net carbonate budgets as the lower bound of carbonate production minus the
211 upper bound of bioerosion (i.e., parrotfish bioerosion \times 50% reincorporation) and, conversely,
212 the upper bound of the net carbonate budgets as the upper bound of carbonate production minus
213 the lower bound of bioerosion (i.e., parrotfish bioerosion \times 50% reincorporation). We therefore
214 determined net carbonate budgets as a categorical variable that was positive if the net carbonate
215 budgets (\pm uncertainties) were greater than zero (i.e., net CaCO_3 production), neutral if the net
216 carbonate budgets (\pm uncertainties) overlapped zero, and negative if the net carbonate budgets
217 (\pm uncertainties) were less than zero (i.e., net CaCO_3 loss).

218 *Chemistry-based net calcification*

219 Differences in coral reef and offshore seawater total alkalinity were used to assess
220 chemistry-based net calcification for each reef site (Langdon et al. 2010; Cyronak et al. 2018).
221 Seawater carbonate chemistry samples were collected via a 5 L Niskin bottle at 0-20 m depth,
222 stored in 500 mL borosilicate glass bottles with a 200 μL saturated mercuric chloride solution,
223 and analyzed for TA (\pm 0.1% uncertainty) following best practices on an open cell potentiometric
224 acid titration system developed by the laboratory of Professor A. Dickson (see (Barkley et al.

225 2021) for further details on data collection). Salinity ($\pm 0.0005 \text{ S m}^{-1}$ uncertainty) was measured
226 in situ via a Seabird Electronics 19+ CTD (2017–2018) or RBR Concerto³ (2019) at the time of
227 sampling (Barkley et al. 2021). Salinity normalized total alkalinity anomalies ($\Delta n\text{TA}$) for each
228 coral reef location were calculated from NOAA Pacific NCRMP offshore and coral reef total
229 alkalinity (TA) data: $\Delta n\text{TA} = n\text{TA}_{\text{offshore}} - n\text{TA}_{\text{reef}}$ (Langdon et al. 2010; Cyronak et al. 2018) so
230 that positive values reflected net calcification and negative values net CaCO_3 dissolution. TA
231 was normalized according to the protocols outlined in (Courtney et al. 2021b). To assess the
232 uncertainties introduced by the salinity normalization calculation and the potential influence of
233 zero salinity end members with a $\text{TA} > 0$, multiple calculations were conducted for a range of
234 potential freshwater TA end members ($\text{TA}_{\text{S}=0} = 15\text{--}1298 \mu\text{mol kg}^{-1}$) and for salinity normalization
235 with respect to both the mean offshore or mean reef salinity (Courtney et al. 2021b). The mean,
236 maximum, and minimum of all $\Delta n\text{TA}_{\text{offshore}}$ and $\Delta n\text{TA}_{\text{reef}}$ values for each cruise and location
237 were then used to determine $\Delta n\text{TA}$ and the associated uncertainties ($\Delta n\text{TA} \pm \text{uncertainties}$).

238 While the magnitude of $\Delta n\text{TA}$ can be used to calculate net coral reef calcification rates if
239 seawater depth and residence time are known, these factors were not quantified as part of the
240 monitoring efforts in this study so the magnitude of $\Delta n\text{TA}$ for each reef only reflects the total
241 change in alkalinity, but not the rate of change. The sign of $\Delta n\text{TA}$ nonetheless elucidates whether
242 the reef system was net calcifying (i.e., positive $\Delta n\text{TA}$) or net CaCO_3 dissolving (i.e., negative
243 $\Delta n\text{TA}$) at the time of measurement. We therefore determined chemistry-based net calcification
244 from the $\Delta n\text{TA}$ for each reef as a categorical variable that was positive if the $\Delta n\text{TA}$
245 ($\pm \text{uncertainties}$) was greater than zero (i.e., net calcifying), neutral if the $\Delta n\text{TA}$ ($\pm \text{uncertainties}$)
246 overlapped zero, and negative if the $\Delta n\text{TA}$ ($\pm \text{uncertainties}$) was less than zero (i.e., net CaCO_3
247 dissolving).

248 *Degree Heating Weeks*

249 Owing to the proximity of the 2014-2017 global coral bleaching event (Eakin et al. 2019)
250 to the 2017-2019 survey dates in this study, we extracted the maximum accumulated degree
251 heating weeks (DHW) at each reef site for each year between 2014 and 2017 to quantify the
252 number of reef sites experiencing ecologically significant ($DHW \geq 4$) or ecologically severe
253 ($DHW \geq 8$) heat stress (Eakin et al. 2010; Heron et al. 2016; Skirving et al. 2019, 2020) from the
254 NOAA Coral Reef Watch DHW v3.1 dataset (NOAA Coral Reef Watch 2018).

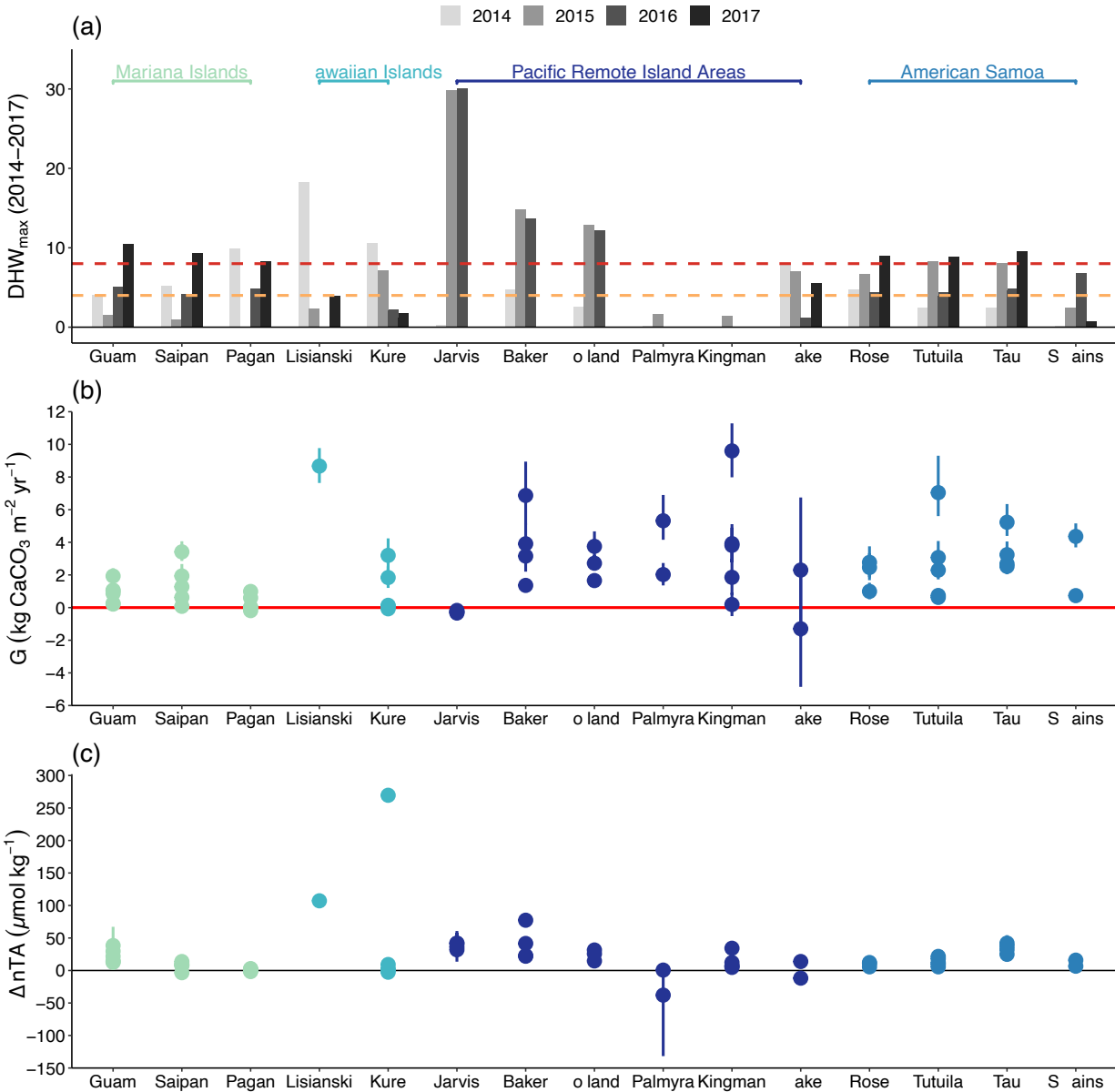
255 *Correlations between coral reef metrics*

256 Linear mixed effects models were used to quantify the relationships between net
257 carbonate budgets, salinity normalized total alkalinity anomalies, percent coral cover, and
258 maximum degree heating weeks experienced during the 2014–2017 global coral bleaching event.
259 Random effects were incorporated to allow the estimated slopes and intercepts for each response
260 variable to vary by island. All models were constructed and evaluated using the *R* package *nlme*
261 (Pinheiro et al. 2019).

262 *Calcification Vulnerability Index*

263 In response to the need for simple, but comprehensive and meaningful metrics of coral
264 reef function and status under global environmental change that offer insight for researchers,
265 managers, and policymakers (NOAA Ocean Acidification Program 2018), we combined the
266 census-based and chemistry-based assessments in a term referred to as the calcification
267 vulnerability index. This index was determined as a categorical variable from the census-based
268 net carbonate budgets and chemistry-based net calcification assessments for each reef.
269 Calcification vulnerability index was therefore positive for reefs with positive net carbonate
270 budgets and net calcification assessments, negative for reefs with negative net carbonate budgets

271 and net calcification assessments, and neutral for any other combination of positive, neutral, or
272 negative net carbonate budgets and net calcification assessments. While there is nonetheless
273 uncertainty in quantifying the maintenance of coral reef CaCO₃ structures from snapshot data,
274 we interpret positive calcification vulnerability index as reefs that are of minimal concern for
275 maintaining their CaCO₃ balance, neutral calcification vulnerability index as reefs that are of
276 moderate concern for maintaining this balance, and negative calcification vulnerability index as
277 reefs that are of imminent concern for maintaining their CaCO₃ balance. We then used Kruskal-
278 Wallis tests to evaluate how well the categorical census-based net carbonate budgets (i.e.,
279 positive, neutral, or negative), categorical chemistry-based net calcification assessments (i.e.,
280 positive, neutral, or negative), and calcification vulnerability index corresponded to the
281 maximum heat stress experienced during the 2014–2017 global coral bleaching event and the
282 commonly used reef condition metric of percent coral cover (Gardner et al. 2003; Bruno and
283 Selig 2007; De’ath et al. 2012). Pairwise comparisons of maximum heat stress and coral cover
284 between positive, neutral, and negative classifications for each metric were then conducted using
285 post hoc Dunn’s Tests with Bonferroni corrections using the statistical package *FSA* (Ogle et al.
286 2021).



287

288 **Figure 3.** (a) Maximum Degree Heating Weeks (DHW) experienced at each island in each year of the 2014–2017
 289 global coral bleaching event. Dashed orange line indicates ecologically significant coral heat stress (4 DHW) and
 290 dashed red line indicates ecologically severe coral heat stress (8 DHW). (b) Net carbonate budget (G) \pm uncertainties
 291 are reported for each site around each island. (c) Salinity normalized total alkalinity anomaly (ΔnTA) \pm uncertainties
 292 are reported for each site around each island. All sites are denoted by the name of the respective island or atoll.

293

294 **Results**

295 *Accumulated Bleaching-relevant Heat Stress 2014-2017*

296 The majority of coral reef sites likely experienced ecologically severe (i.e., $DHW \geq 8$)
297 heat stress (i.e., 79% of reef sites; $n=44$; $DHW \geq 8$) at some point during the 2014–2017 coral
298 bleaching event with multiple years of bleaching-level stress recorded in the remotely sensed
299 data (Figure 3a). While we refer to the accumulated heat stress from 2014–2017 as the global
300 coral bleaching event following (Eakin et al. 2019), we acknowledge that many reefs in this
301 study experienced multiple years with projected bleaching level heat stress suggesting this was a
302 series of bleaching events for many locations (Figure 3a). Additional reef sites around the islands
303 of Wake, Swains, and Tutuila likely experienced ecologically significant (i.e., $DHW \geq 4$) heat
304 stress (i.e., 9% of reef sites; $n=5$; $4 \leq DHW \leq 8$; Figure 3a). The islands of Kingman and Palmyra
305 in the Pacific Remote Island Areas harbored the only sites (i.e., 13% of reef sites; $n=7$) that likely
306 did not experience ecologically significant heat stress (i.e., $DHW < 4$) during the 2014–2017
307 coral bleaching event (Figure 3a).



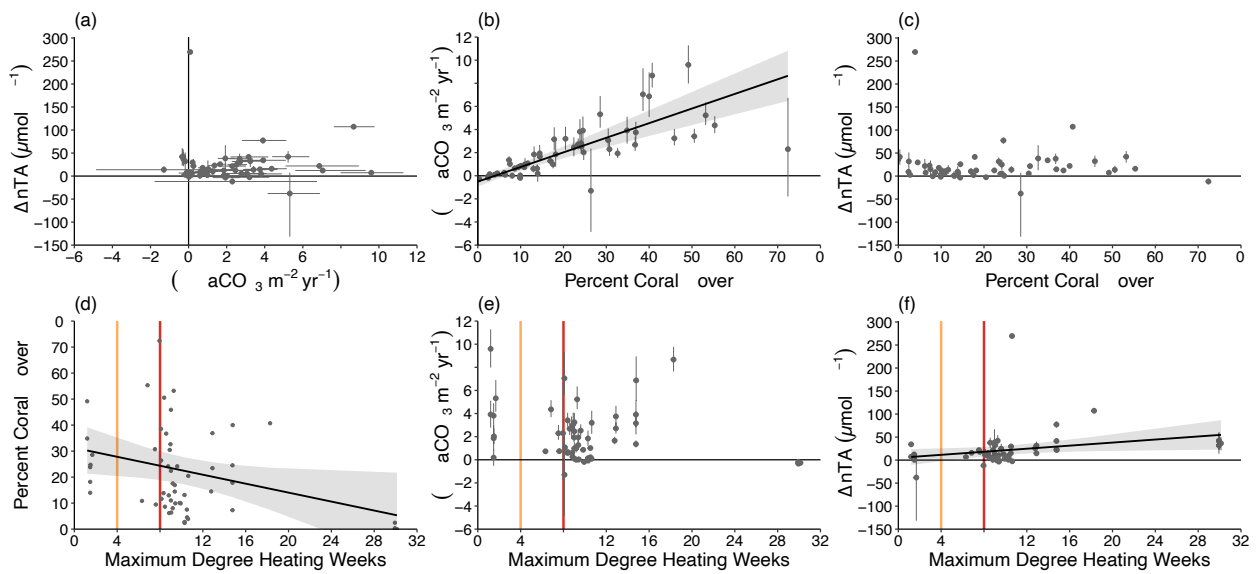
308
 309 **Figure 4.** The number of reef sites classified as having either positive, neutral, or negative (a) census-based net
 310 carbonate budget, (b) chemistry-based net calcification, and (c) calcification vulnerability index are reported for
 311 each island within the Mariana Islands, Northwestern Hawaiian Islands, Pacific Remote Island Areas, and American
 312 Samoa. All sites are denoted by the name of the respective island or atoll.

313
 314 *Coral Reef Calcification Metrics*

315 The mean ($\pm 95\%$) of site-level census-based net carbonate budgets was 2.1 ± 0.6 kg
 316 $\text{CaCO}_3 \text{ m}^{-2} \text{ yr}^{-1}$ (range = -1.3 to $9.6 \text{ kg CaCO}_3 \text{ m}^{-2} \text{ yr}^{-1}$) (Figure 3b) with 43 reef sites exhibiting
 317 net positive carbonate budgets, 9 sites exhibiting neutral net carbonate budgets, and 4 sites

318 exhibiting net negative carbonate budgets (Figure 4a). The mean ($\pm 95\%$) of site-level chemistry-
 319 based salinity normalized alkalinity anomalies was $22 \pm 10 \mu\text{mol kg}^{-1}$ (range = -38 to $270 \mu\text{mol}$
 320 kg^{-1}) (Figure 3c) with 47 sites exhibiting positive net calcification, 6 sites exhibiting neutral net
 321 calcification, and 3 sites exhibiting negative net calcification (Figure 4b). Calcification
 322 vulnerability index was positive for 38 reef sites, neutral for 18 reef sites, and negative for 0 reef
 323 sites (Figure 4c).

324



325

326 **Figure 5.** Site-level correlations between census-based net carbonate budgets (G), chemistry-based salinity
 327 normalized total alkalinity anomalies (ΔnTA), percent coral cover, and maximum degree heating weeks. (a) ΔnTA is
 328 evaluated as a function of G , (b) G is evaluated as a function of percent coral cover, and (c) ΔnTA is evaluated as a
 329 function of percent coral cover. (d, e, f) Maximum degree heating weeks refers to the maximum accumulated degree
 330 heating weeks experienced during the 2014-2017 global coral bleaching event. (d) Percent coral cover, (e) G , and (f)
 331 ΔnTA were each evaluated as a function of maximum degree heating weeks. Linear regressions ($\pm 95\%$) are plotted
 332 for linear mixed effects models for all slopes with $p < 0.05$. The vertical orange line indicates ecologically significant
 333 coral heat stress (4 DHW) and vertical red line indicates ecologically severe coral heat stress (8 DHW).

334

335 *Correlations Between Coral Reef Metrics*

336 There were no detectable correlations between site-level ΔnTA and G ($p=0.929$), ΔnTA
337 and percent coral cover ($p=0.551$), and G and maximum DHW ($p=0.430$) (Figure 5). In contrast,
338 positive correlations were observed between G and percent coral cover (slope = 0.13 G per %
339 coral cover; $p<0.001$) and ΔnTA and maximum DHW (slope = 1.66 $\mu\text{mol/kg}$ per DHW;
340 $p=0.044$) (Table S2). A negative correlation was observed between coral cover and maximum
341 DHW (slope = -0.86 % coral cover per DHW; $p=0.042$). The threshold for maintaining positive
342 net carbonate budgets was $8.6\pm 6.0\%$ from the linear mixed effects models (Figure 4b, Table S2).

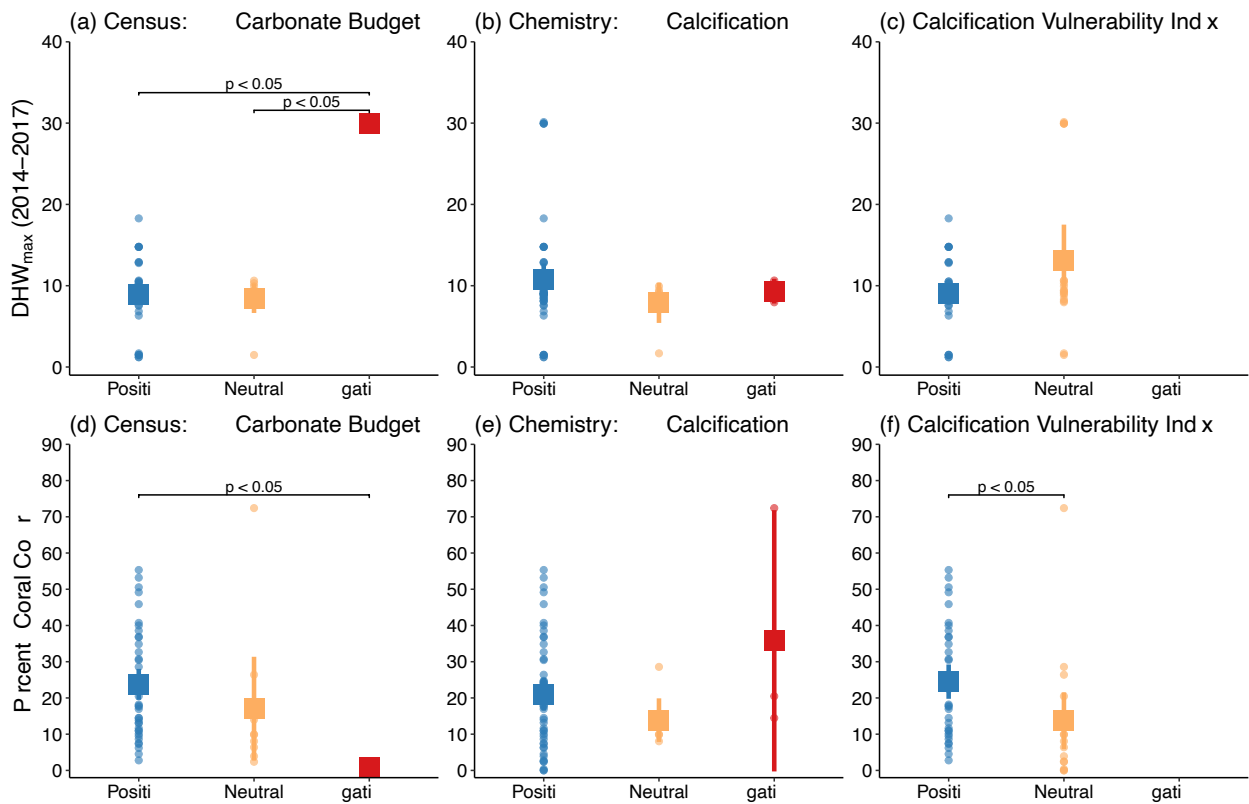
343

344 *Degree Heating Weeks and Coral Cover as Predictors of Coral Reef Calcification Metrics*

345 There were detectable differences in maximum DHW experienced during the 2014–2017
346 coral bleaching event between positive, neutral, and negative net carbonate budgets (Kruskal-
347 Wallis Test, $p<0.004$) with higher maximum DHW for negative net carbonate budgets than
348 positive (Dunn's Test, $p=0.003$, Figure 6a) and neutral (Dunn's Test, $p=0.014$, Figure 6a) net
349 carbonate budgets. Conversely, there were no detectable differences in maximum DHW
350 experienced during the 2014–2017 coral bleaching event between classifications of chemistry-
351 based net calcification estimates (Kruskal-Wallis Test, $p=0.780$, Figure 6b) or calcification
352 vulnerability index (Kruskal-Wallis Test, $p=0.243$, Figure 6c).

353 There were detectable differences in coral cover between positive, neutral, and negative
354 net carbonate budgets (Kruskal-Wallis Test, $p<0.001$) with lower coral cover for reefs with
355 negative net carbonate budgets compared to positive net carbonate budgets (Dunn's Test,
356 $p=0.001$), with no detectable differences in coral cover between reefs with negative net carbonate
357 budgets compared to neutral net carbonate budgets (Dunn's Test, $p=0.193$) or neutral net
358 carbonate budgets compared to positive net carbonate budgets (Dunn's Test, $p=0.157$) (Figure

359 6d). Conversely, there were no detectable differences in coral cover between net calcification
 360 classifications (Kruskal-Wallis Test, $p=0.381$) (Figure 6e). Lastly, we observed detectable
 361 differences in coral cover between classifications of calcification vulnerability index (Kruskal-
 362 Wallis Test, $p=0.003$) with greater coral cover at positive calcification vulnerability index sites
 363 compared to sites with a neutral (Dunn's Test, $p=0.003$) calcification vulnerability index. There
 364 were no sites with a negative calcification vulnerability index (Figure 6f).



365
 366 **Figure 6.** Maximum degree heating weeks (DHW) experienced during the 2014-2017 global coral bleaching event
 367 are reported for positive, neutral, and negative classifications of the (a) census-based net carbonate budget, (b)
 368 chemistry-based net calcification, and (c) calcification vulnerability index as circles for each coral reef. Percent coral
 369 cover is reported for positive, neutral, and negative classifications of the (d) census-based net carbonate budget, (e)
 370 chemistry-based net calcification, and (f) calcification vulnerability index as circles for each coral reef. Mean ± 95%
 371 maximum DHW and percent coral cover are plotted as squares with line range on top of the site level circles for
 372 each category. Horizontal pairwise comparisons above the categorical variables represent statistical significance at

373 the $\alpha=0.05$ level from post hoc Dunn's Tests with Bonferroni Corrections conducted on Kruskal-Wallis Tests of
374 maximum DHW and percent coral cover, respectively, vs. the coral reef calcification metric in each panel.

375

376 *Site-level coral reef summary data*

377 In addition to the primary analyses presented here, site-level benthic community
378 composition, seawater carbonate chemistry data, census-based net carbonate budgets, chemistry-
379 based net calcification estimates (i.e., salinity normalized total alkalinity anomalies),
380 calcification vulnerability index, and maximum DHW experienced for each of the 56 coral reefs
381 in this study are available in the supplementary material (Table S3).

382

383 Discussion

384 While the majority of the Pacific Ocean reef sites investigated here most likely
385 experienced ecologically severe ($n=44$, 79% of total) or significant ($n=5$, 9% of total) heat stress,
386 mean ($\pm 95\%$) census-based net carbonate production ($G=2.1\pm 0.6$ kg CaCO_3 m^{-2} yr^{-1}) and
387 chemistry-based net calcification ($\Delta n\text{TA}=22\pm 10$ $\mu\text{mol kg}^{-1}$) were positive in this study (Figure
388 3). Moreover, 77% ($n=43$ sites) of coral reef locations exhibited positive net carbonate budgets
389 while positive net calcification states were observed for 84% ($n=47$ reefs) of coral reef locations
390 (Figure 4). The combined census-based and chemistry-based calcification vulnerability index
391 suggests that all reef sites were therefore classified as minimal (68%, $n=38$ sites) to moderate
392 (32%, $n=18$ sites) concern for maintaining their CaCO_3 balance (Figure 4) at the time of
393 observation in the years following the global bleaching event. However, some caution is advised
394 in interpreting these results, as we do not know how these properties changed in response to the
395 bleaching event. Regardless, at the time of the observations it can be concluded that more than
396 half of the reefs surveyed showed a positive CaCO_3 balance from both a census-based and

397 chemistry based perspective, but that many coral reefs may be approaching a potential tipping
398 point for maintaining calcium carbonate structures and accretion under ongoing and future
399 climate change. The metrics presented here assess concern for maintaining CaCO₃ balance based
400 on census and chemistry-based approaches; however, the question remains whether thresholds
401 other than zero may be more relevant to the sustained geo-ecological function of coral reefs? The
402 mean net carbonate budgets in this study were low (mean±95%=2.1±0.6 kg CaCO₃ m⁻² yr⁻¹)
403 supporting the notion that reefs may be unable to keep up with accelerating sea level rise under
404 higher CO₂ emissions scenarios (Perry et al. 2018a), especially when taking into account the
405 additional role of chemical CaCO₃ dissolution and physical transport processes that were omitted
406 from the census-based methods (Browne et al. 2021). Additionally, these assessments of concern
407 for maintaining reef's CaCO₃ balances are based on the present assessment and do not take into
408 account the future stressors on net carbonate budgets caused by increases in coral bleaching
409 events, coral disease outbreaks, and CaCO₃ dissolution rates (Van Hooidonk et al. 2016; Randall
410 and van Woesik 2017; Eyre et al. 2018).

411 The present observations of calcification metrics were made after the 2014-2017 global
412 coral bleaching event with no direct estimations of coral reef calcification metrics before the heat
413 stress event so the underlying mechanism for any associations between DHW experienced and
414 the calcification metrics in this study remain equivocal. Nonetheless, coral cover was negatively
415 correlated with maximum DHW during the 2014–2017 global coral bleaching event (Figure 5d),
416 which is consistent with observations of widespread coral mortality observed in these regions
417 during this anomalous warm period (Reynolds et al. 2014; Couch et al. 2017; Vargas-Ángel et al.
418 2019). At the island scale, Jarvis experienced repeated years with DHW>30 (Figure 3a), high
419 coral mortality during the 2014-2017 coral bleaching event (Vargas-Ángel et al. 2019), and was

420 the only island in this study with negative net carbonate budgets (Figure 3b, 4a). While there was
421 no detectable trend between census-based net carbonate budgets and maximum DHW (Figure
422 5e), reefs with negative net carbonate budgets did experience greater maximum DHW than reefs
423 with positive or neutral net carbonate budgets (Figure 6a). Collectively, this evidence suggests
424 heat stress may have decreased net carbonate budgets owing to bleaching induced coral mortality
425 from elevated heat stress (Figure 3,5). Notably, there was a positive correlation between ΔnTA
426 and maximum DHW (Figure 5f), with Jarvis maintaining positive chemistry-based net
427 calcification despite experiencing extensive coral mortality (Figure 3). While we lack the data to
428 rigorously explain this seemingly paradoxical correlation between ΔnTA and DHW, there was
429 no difference in maximum DHW between positive, neutral, and negative ΔnTA classifications
430 (Figure 6b). Thus, the sign of net calcification states did not correlate with maximum DHW and,
431 instead, only the magnitude of ΔnTA was correlated with maximum DHW. We posit that longer
432 seawater residence times could account for a greater accumulation of DHW during the coral
433 bleaching event owing to local amplification of warming (*sensu* (DeCarlo et al. 2017)) and
434 greater ΔnTA owing to longer times for calcifiers to modify the overlying seawater (Courtney
435 and Andersson 2019); however, this remains speculative as we lack the information to rigorously
436 investigate this finding with the currently available data.

437 There was no detectable relationship between census-based net carbonate budgets and
438 chemistry-based salinity normalized total alkalinity anomalies (Figure 5a), which resulted in a
439 slight mismatch between the sign of net carbonate budgets and net calcification within each focal
440 region (Figure 4). This is not entirely unexpected since census-based net carbonate budgets (i.e.,
441 carbonate production – bioerosion) and chemistry-based net calcification (i.e., calcification –
442 $CaCO_3$ dissolution) quantify different processes integrating over different spatial and temporal

443 scales (Figure 1). For example, physical aspects of bioerosion may not necessarily lead to
444 chemical CaCO_3 dissolution that would be detected by chemical measurements, and, conversely,
445 sources of CaCO_3 dissolution are not directly accounted for in the census-based carbonate
446 budgets. In particular, the omittance of chemical CaCO_3 dissolution in microenvironments within
447 the reef framework and sediments is a common limitation of census-based carbonate production
448 estimates and can be a significant driver capable of shifting reefs with otherwise calcifying
449 communities to net CaCO_3 dissolution (Tribble et al. 1990; Andersson et al. 2009; Cyronak et al.
450 2013). Additionally, mismatches in temporal scales between the annualized estimates of
451 carbonate production estimates and nearly instantaneous measurements of net calcification by
452 chemistry-based methods could further decouple estimates of net carbonate budgets and net
453 calcification (Figure 1). For example, coral reef TA samples in this study were primarily
454 collected during daylight hours (Figure S1), which would tend to bias measurements towards net
455 calcification (Cyronak et al. 2018). Moreover, differences in hydrodynamics between sites have
456 significant capacity to decouple rates of benthic calcification from the magnitude of salinity
457 normalized total alkalinity anomalies primarily owing to differences in seawater residence times
458 and depth between locations (Cyronak et al. 2018; Courtney and Andersson 2019). The process
459 of salinity normalization itself may also impart some additional uncertainties (Courtney et al.
460 2021b), especially in the case of Palmyra Atoll in this study, which experienced the largest
461 salinity difference between the reef and offshore and negative net calcification (e.g., see larger
462 ΔnTA uncertainties for Palmyra in Figure 3c). (Koweek et al. 2015) observed variable net
463 calcification rates with high rates of calcification observed during the daytime with periods of
464 nighttime dissolution at Palmyra Atoll, suggesting a combination of nighttime dissolution and/or
465 entrainment of lagoon water likely led to the negative ΔnTA observed for Palmyra in this study.

466 This apparent contradiction highlights the value of collecting seawater TA samples over a full
467 diel cycle and/or for extended periods of time while also avoiding sampling over large salinity
468 ranges to reduce uncertainties in chemistry-based net calcification measurements. In contrast, the
469 net carbonate budgets in this study are also somewhat limited by the use of top-down imagery,
470 which does not account for additional sources of calcification or CaCO₃ dissolution hidden
471 beneath the overlying canopy (Goatley and Bellwood 2011; Courtney et al. 2016), and mean
472 (\pm uncertainty) annualized calcification and bioerosion rates from the literature, which does not
473 account for systematic spatiotemporal variability in these sources of carbonate production and
474 loss (Lange et al. 2020a). The categorical metrics were not always in direct agreement in this
475 study, but the calcification vulnerability index more closely followed the census-based net
476 carbonate budgets than the chemistry-based net calcification assessment (Figure 4). While this
477 might suggest that the chemistry-based metric provides little additional information, we conclude
478 that assessing vulnerability of coral reefs to maintain their CaCO₃ balance through multiple lines
479 of evidence increases confidence in our assessment while providing different time perspectives
480 of a chronic vs. acute condition (Figure 1) that integrate over varying spatial scales. Tracking
481 changes in simplified net carbonate budgets and salinity normalized total alkalinity anomalies
482 through time within each reef system using directly comparable methods may also provide more
483 quantitative evidence of changes in calcification states through time (Figure 1).

484 Traditionally, studies have monitored long-term changes in coral cover as a metric for
485 coral reef condition (Gardner et al. 2003; Bruno and Selig 2007; De'ath et al. 2012). While field-
486 based evidence for the correlation between coral cover and net calcification in chemistry-based
487 studies is lacking (Courtney and Andersson 2019), overall coral cover is generally correlated
488 with net carbonate production in census-based studies (Perry et al. 2013, 2015; Januchowski-

489 Hartley et al. 2017). However, net carbonate production rates can nonetheless vary between reef
490 systems of similar coral cover owing to differences in the relative abundances of coral taxa with
491 varying calcification rates (Perry et al. 2015; Januchowski-Hartley et al. 2017; Courtney et al.
492 2020) and differences in the relative abundance of scraping, excavating, and browsing
493 parrotfishes (Januchowski-Hartley et al. 2017; Lange et al. 2020a). Nonetheless, previous net
494 carbonate budget studies have suggested that $\geq 10\%$ coral cover may be a suitable threshold for
495 the maintenance of positive carbonate production states in the Caribbean (Perry et al. 2013), $\sim 2\%$
496 for *Acropora* dominated reefs and $\sim 12.5\%$ for *Porites/Pocillopora* dominated reefs in the
497 Chagos Archipelago (Perry et al. 2015), and 11-18% coral cover in the Seychelles depending on
498 the relative abundances of excavating parrotfishes (Januchowski-Hartley et al. 2017). In this
499 study, we observed a positive correlation between net carbonate budgets and coral cover (Figure
500 5b) with a threshold coral cover of $8.6 \pm 6.0\%$ for maintaining positive net carbonate budgets
501 (Figure 5b, Table S2). We posit that this slightly lower threshold for maintaining positive net
502 carbonate budgets was likely due to the high abundance of framework building corals across the
503 Pacific Ocean (Darling et al. 2019), potential differences in parrotfish functional groups
504 (Januchowski-Hartley et al. 2017; Lange et al. 2020a), and the 50% reincorporation rate of
505 parrotfish bioerosion applied here that was not used in the former studies (Perry et al. 2013,
506 2015; Januchowski-Hartley et al. 2017). For example, the large uncertainties in net carbonate
507 budgets for Wake Atoll were owing to a few observations of *Bolbometopon muricatum*, which
508 are responsible for anomalously high estimates of bioerosion (Perry et al. 2018b). Consequently,
509 we found that coral reefs with positive net carbonate budgets had significantly higher coral cover
510 than reefs with negative net carbonate budgets (Figure 6d). No relationship was observed
511 between coral cover and ΔnTA in this study (Figure 5c, 6e; but see the above discussion of coral

512 reef carbonate production estimates and alkalinity anomalies). Coral cover was greater for coral
513 reefs with a positive combined census-based and chemistry-based calcification vulnerability
514 index compared to neutral classifications (Figure 6f). Reefs with a neutral calcification
515 vulnerability index had a mean ($\pm 95\%$) coral cover of $13.7 \pm 7.9\%$, which is in remarkable
516 agreement with the 2-18% previously established thresholds for net carbonate budget tipping
517 points (Perry et al. 2013, 2015; Januchowski-Hartley et al. 2017) despite being based on both
518 census-based and chemistry-based methods.

519 However, there was considerable variability in coral cover among sites with a neutral
520 calcification vulnerability index and we also observed a wide range of coral cover for sites with a
521 positive calcification vulnerability index with coral cover less than 10% for many of those sites
522 (Figure 6). These findings highlight the nuance and uncertainties associated with using a
523 simplified coral cover threshold as a proxy for assessing the capacity for reefs to maintain
524 CaCO_3 structures. Crustose coralline algae and other calcifying organisms are likely to become
525 increasingly important contributors for maintaining CaCO_3 structures in low coral cover ($<10\%$)
526 or recently bleached coral reef systems (Kayanne et al. 2005; Courtney et al. 2018). For example,
527 the 12-28% cover of crustose coralline algae at Jarvis in this study may have maintained positive
528 alkalinity anomalies indicative of a net calcifying reef state despite 0 to 2.5% coral cover at the
529 time of the surveys (Figure 3, Table S1). Coupled with the evidence that CCA may be increasing
530 following mass bleaching events on certain reefs in the equatorial Pacific (Pacific Islands
531 Fisheries Science Center 2021), these findings support the need to further assess the role of
532 crustose coralline algae and other non-scleractinian coral calcifiers in maintaining positive net
533 carbonate budgets and net calcification for low coral cover reefs ($<10\%$) (Courtney et al. 2018).

534 As the climate crisis continues, robust time series measurements of coral reef status and
535 capacity to maintain carbonate structures will become increasingly important to evaluate the
536 current and projected maintenance of coral reef structures and the associated ecosystem services
537 they provide to humanity. The automated annotation of benthic community composition from
538 imagery via *CoralNet* substantially reduces the efforts to generate sustained time series data and
539 is already producing accurate and traceable classification of benthic communities (Williams et al.
540 2019) with the additional capacity to quantify benthic carbonate production (Chan et al. 2021).
541 We project that these estimates will only continue to improve with the development of location-
542 specific calcification and bioerosion rates from in situ measurements and application of deep
543 learning algorithms to directly assess substrate-specific and entire reef volume changes from
544 repeated three-dimensional coral reef models derived from structure from motion (SfM) (see also
545 (Lange et al. 2020a)). Moreover, snapshots such as the data presented in the current study
546 provide nearly instantaneous evidence to evaluate net calcification states, but alone are unable to
547 capture any changes in coral reef calcification state through time (i.e., increasing, constant, or
548 decreasing) that are essential information for developing any potential intervention strategies.
549 Sustained long-term ecological and biogeochemical monitoring of coral reef state variables such
550 as the calcification metrics presented in this study will therefore prove useful for monitoring the
551 vulnerability of coral reefs to sustain carbonate structures through time to inform evidence-based
552 management of coral reefs and their associated ecosystem services in the Anthropocene.

553

554 Acknowledgments

555 We are grateful for the constructive comments and feedback that Dr. Ines Lange and an
556 anonymous reviewer provided to clarify terminology and improve the synthesis work presented

557 here. TAC, SC, DJK, and AJA were funded by the National Oceanographic and Atmospheric
558 Administration Ocean Acidification Program (NA15OAR4320071). Benthic community, fish
559 community, and carbonate chemistry data collection were funded by the NOAA Coral Reef
560 Conservation Program and NOAA Ocean Acidification Program, as part of the Pacific-National
561 Coral Reef Monitoring Program. All computer code required to generate the analyses herein is
562 currently privately accessible on Figshare (<https://figshare.com/s/01af29a8c92f0a51535b>) and
563 will be made publicly accessible via Zenodo. All data are currently publicly available in the cited
564 data repositories. On behalf of all authors, the corresponding author declares that there are no
565 conflicts of interest.

566

567 Supplementary Materials

568 **Figure S1.** Site-level salinity normalized total alkalinity anomalies (ΔnTA) are plotted relative to the local time of
569 sampling the coral reef seawater total alkalinity water.

570

571 **Table S1.** Species-level bioerosion rates and length-scaling coefficients for parrotfishes observed across the Pacific
572 Ocean in this study. Species represents the respective species name, data represents the source of the originating data
573 source, substitution describes any required substitutions for species lacking in the *ReefBudget* methodology, each
574 size bin represents the bioerosion rate ($\text{kg CaCO}_3 \text{ ind}^{-1} \text{ y}^{-1}$) for the respective fish length (cm) of initial and terminal
575 phase fishes, and a and b represent allometric scaling coefficients of bioerosion for parrotfish length data:

576 Bioerosion ($\text{kg CaCO}_3 \text{ ind}^{-1} \text{ y}^{-1}$) = $a \times TL^b$.

577

578 **Table S2.** Summary statistics are provided for the linear mixed effects model output. For each model (denoted in
579 bold text in the first row), the table reports the estimates \pm 95% and p-values for the respective coefficients, a
580 summary of the random effects, the number of observations, and the resulting R^2 of the model.

581

582 **Table S3.** Site-level summary data are provided for each of the 56 coral reef sites presented in this study including:
583 sample meta-data, summary of benthic community composition, benthic carbonate production, parrotfish bioerosion,
584 net carbonate budgets, salinity normalized total alkalinity anomalies, categorical reef condition metrics, and degree
585 heating weeks associated with the 2014-2017 global coral bleaching event.

586

587 References

588 Andersson, A. J., I. B. Kuffner, F. T. Mackenzie, P. L. Jokiel, K. S. Rodgers, and A. Tan. 2009.

589 Net Loss of CaCO₃ from a subtropical calcifying community due to seawater

590 acidification: mesocosm-scale experimental evidence. *Biogeosciences* **6**: 1811–1823.

591 doi:10.5194/bg-6-1811-2009

592 Aronson, R. B., and W. F. Precht. 2001. White-band disease and the changing face of Caribbean

593 coral reefs, p. 25–38. *In* J.W. Porter [ed.], *The Ecology and Etiology of Newly Emerging*

594 *Marine Diseases*. Springer Netherlands.

595 Ayotte, P., K. McCoy, I. Williams, and J. Zamzow. 2011. Coral Reef Ecosystem Division

596 Standard Operating Procedures: Data Collection for Rapid Ecological Assessment Fish

597 Surveys. *Pac. Isl. Fish. Sci. Cent.* 24.

598 Barkley, H. C., A. A. Halperin, J. N. Smith, R. Weible, and N. Pomeroy. 2021. National Coral

599 Reef Monitoring Program — Ocean Acidification Monitoring of Pacific US Coral Reefs,

600 Coral Reef Carbonate Chemistry of Pacific Remote Island Areas, from 2018-06-08 to

601 2018-08-12 (Accession 225980) (NCEI Accession 0225980). NOAA Natl. Cent. Environ.

602 Inf. <https://www.ncei.noaa.gov/archive/accession/0225980>.

603 Beijbom, O., P. J. Edmunds, C. Roelfsema, and others. 2015. Towards Automated Annotation of

604 Benthic Survey Images: Variability of Human Experts and Operational Modes of

605 Automation. *PLOS ONE* **10**: e0130312. doi:10.1371/journal.pone.0130312

606 Berg, P., H. Røy, and P. L. Wiberg. 2007. Eddy correlation flux measurements: The sediment
607 surface area that contributes to the flux. *Limnol. Oceanogr.* **52**: 1672–1684.
608 doi:10.4319/lo.2007.52.4.1672

609 Broecker, W. S., and T. Takahashi. 1966. Calcium carbonate precipitation on the Bahama Banks.
610 *J. Geophys. Res.* **71**: 1575. doi:10.1029/JZ071i006p01575

611 Browne, N. K., M. Cuttler, K. Moon, and others. 2021. Predicting Responses of Geo-ecological
612 Carbonate Reef Systems to Climate Change: A Conceptual Model and Review, *In*
613 *Oceanography and Marine Biology*. CRC Press.

614 Bruno, J. F., and E. R. Selig. 2007. Regional decline of coral cover in the Indo-Pacific: Timing,
615 extent, and subregional comparisons. *PLoS ONE* **2**: e711.
616 doi:10.1371/journal.pone.0000711

617 Chan, S., T. Courtney, A. Andersson, and D. Kriegman. 2021. CoralNet now estimates carbonate
618 production rates. *CoralNet*.

619 Chave, K. E., S. V. Smith, and K. J. Roy. 1972. Carbonate production by coral reefs. *Mar. Geol.*
620 **12**: 123–140. doi:10.1016/0025-3227(72)90024-2

621 Chisholm, J. R. M., and J. Gattuso. 1991. Validation of the alkalinity anomaly technique for
622 investigating calcification of photosynthesis in coral reef communities. *Limnol.*
623 *Oceanogr.* **36**: 1232–1239. doi:10.4319/lo.1991.36.6.1232

624 Couch, C. S., J. H. R. Burns, G. Liu, K. Steward, T. N. Gutlay, J. Kenyon, C. M. Eakin, and R.
625 K. Kosaki. 2017. Mass coral bleaching due to unprecedented marine heatwave in
626 Papahānaumokuākea Marine National Monument (Northwestern Hawaiian Islands).
627 *PLOS ONE* **12**: e0185121. doi:10.1371/journal.pone.0185121

628 Courtney, T. A., and A. J. Andersson. 2019. Evaluating measurements of coral reef net
629 ecosystem calcification rates. *Coral Reefs* **38**: 997–1006. doi:10.1007/s00338-019-01828-
630 2

631 Courtney, T. A., A. J. Andersson, N. R. Bates, and others. 2016. Comparing Chemistry and
632 Census-Based Estimates of Net Ecosystem Calcification on a Rim Reef in Bermuda.
633 *Front. Mar. Sci.* **3**: 181. doi:10.3389/fmars.2016.00181

634 Courtney, T. A., B. B. Barnes, I. Chollett, and others. 2020. Disturbances drive changes in coral
635 community assemblages and coral calcification capacity. *Ecosphere* **11**: e03066.
636 doi:10.1002/ecs2.3066

637 Courtney, T. A., E. H. D. Carlo, H. N. Page, and others. 2018. Recovery of reef-scale
638 calcification following a bleaching event in Kāneʻohe Bay, Hawaiʻi. *Limnol. Oceanogr.*
639 *Lett.* **3**: 1–9. doi:10.1002/lo12.10056

640 Courtney, T. A., S. Chan, I. D. Lange, C. T. Perry, D. J. Kriegman, and A. J. Andersson. 2021a.
641 Area-normalized scaling of ReefBudget calcification, macrobioerosion, and
642 microbioerosion rates for use with CoralNet Version 1.0, Zenodo,
643 <https://zenodo.org/record/5140477>.

644 Courtney, T. A., T. Cyronak, A. J. Griffin, and A. J. Andersson. 2021b. Implications of salinity
645 normalization of seawater total alkalinity in coral reef metabolism studies. *PLOS ONE*
646 **16**: e0261210. doi:10.1371/journal.pone.0261210

647 Cyronak, T., A. J. Andersson, C. Langdon, and others. 2018. Taking the metabolic pulse of the
648 world's coral reefs. *PLOS ONE* **13**: e0190872. doi:10.1371/journal.pone.0190872

649 Cyronak, T., I. R. Santos, and B. D. Eyre. 2013. Permeable coral reef sediment dissolution
650 driven by elevated pCO₂ and pore water advection. *Geophys. Res. Lett.* **40**: 4876–4881.
651 doi:10.1002/grl.50948

652 Darling, E. S., T. R. McClanahan, J. Maina, and others. 2019. Social–environmental drivers
653 inform strategic management of coral reefs in the Anthropocene. *Nat. Ecol. Evol.* **3**:
654 1341–1350. doi:10.1038/s41559-019-0953-8

655 De’ath, G., K. E. Fabricius, H. Sweatman, and M. Puotinen. 2012. The 27-year decline of coral
656 cover on the Great Barrier Reef and its causes. *Proc. Natl. Acad. Sci. U. S. A.* **109**:
657 17995–9. doi:10.1073/pnas.1208909109

658 DeCarlo, T. M., A. L. Cohen, G. T. F. Wong, K. A. Davis, P. Lohmann, and K. Soong. 2017.
659 Mass coral mortality under local amplification of 2 °C ocean warming. *Sci. Rep.* **7**:
660 44586. doi:10.1038/srep44586

661 Eakin, C. M., J. A. Morgan, S. F. Heron, and others. 2010. Caribbean Corals in Crisis: Record
662 Thermal Stress, Bleaching, and Mortality in 2005. *PLOS ONE* **5**: e13969.
663 doi:10.1371/journal.pone.0013969

664 Eakin, C. M., H. P. A. Sweatman, and R. E. Brainard. 2019. The 2014–2017 global-scale coral
665 bleaching event: insights and impacts. *Coral Reefs* **38**: 539–545. doi:10.1007/s00338-
666 019-01844-2

667 Eyre, B. D., T. Cyronak, P. Drupp, E. H. D. Carlo, J. P. Sachs, and A. J. Andersson. 2018. Coral
668 reefs will transition to net dissolving before end of century. *Science* **359**: 908–911.
669 doi:10.1126/science.aao1118

670 Gardner, T. A., I. M. Cote, J. A. Gill, and others. 2003. Long-Term Region-Wide Declines in
671 Caribbean Corals. *Science* **301**: 958–960. doi:10.1038/020493a0

672 Goatley, C. H. R., and D. R. Bellwood. 2011. The roles of dimensionality, canopies and
673 complexity in ecosystem monitoring. *PLoS ONE* **6**: e27307.
674 doi:10.1371/journal.pone.0027307

675 Heenan, A., I. D. Williams, T. Acoba, A. DesRochers, R. K. Kosaki, T. Kanemura, M. O.
676 Nadon, and R. E. Brainard. 2017. Long-term monitoring of coral reef fish assemblages in
677 the Western central pacific. *Scientific Data* **4**:170176.

678 Heron, S. F., L. Johnston, G. Liu, and others. 2016. Validation of Reef-Scale Thermal Stress
679 Satellite Products for Coral Bleaching Monitoring. *Remote Sens.* **8**: 59.
680 doi:10.3390/rs8010059

681 Hubbard, D. K., A. I. Miller, and D. Scaturro. 1990. Production and cycling of calcium carbonate
682 in a shelf-edge reef system (St. Croix, U.S. Virgin Islands): Applications to the nature of
683 reef systems in the fossil record,.

684 Januchowski-Hartley, F. A., N. A. J. Graham, S. K. Wilson, and others. 2017. Drivers and
685 predictions of coral reef carbonate budget trajectories. doi:10.1098/rspb.2016.2533

686 Kayanne, H., H. Hata, S. Kudo, and others. 2005. Seasonal and bleaching-induced changes in
687 coral reef metabolism and CO₂ flux. *Glob. Biogeochem. Cycles* **19**: 1–11.
688 doi:10.1029/2004GB002400

689 Kleypas, J. A., R. W. Buddemeier, and J. P. Gattuso. 2001. The future of coral reefs in an age of
690 global change. *Int. J. Earth Sci.* **90**: 426–437. doi:10.1007/s005310000125

691 Kowweek, D., R. B. Dunbar, J. S. Rogers, G. J. Williams, N. Price, D. Mucciarone, and L. Teneva.
692 2015. Environmental and ecological controls of coral community metabolism on Palmyra
693 Atoll. *Coral Reefs* **34**: 339–351. doi:10.1007/s00338-014-1217-3

694 Langdon, C., J.-P. Gattuso, and A. Andersson. 2010. Measurements of calcification and
695 dissolution of benthic organisms and communities U. Riebesell, V. Fabry, L. Hansson,
696 and J. Gattuso [eds.]. Guide Best Pract. Ocean Acidif. Res. Data Report. 213–232.

697 Lange, I. D., C. T. Perry, and L. Alvarez-Filip. 2020a. Carbonate budgets as indicators of
698 functional reef “health”: A critical review of data underpinning census-based methods
699 and current knowledge gaps. *Ecol. Indic.* **110**: 105857.
700 doi:10.1016/j.ecolind.2019.105857

701 Lange, I. D., C. T. Perry, K. M. Morgan, R. Roche, C. E. Benkwitt, and N. A. Graham. 2020b.
702 Site-Level Variation in Parrotfish Grazing and Bioerosion as a Function of Species-
703 Specific Feeding Metrics. *Diversity* **12**: 379. doi:10.3390/d12100379

704 Lowe, R. J., and J. L. Falter. 2015. Oceanic Forcing of Coral Reefs. *Annu. Rev. Mar. Sci.* **7**: 43–
705 66. doi:10.1146/annurev-marine-010814-015834

706 Lozada-Misa, P., B. D. Schumacher, and B. Vargas-Angel. 2017. Analysis of benthic survey
707 images via CoralNet: a summary of standard operating procedures and guidelines, H-17-
708 02. 175. doi:10.7289/V5/AR-PIFSC-H-17-02

709 NOAA Coral Reef Watch. 2018. NOAA Coral Reef Watch Version 3.1 Daily Global 5km
710 Satellite Coral Bleaching Degree Heating Week Product, Jun. 3, 2013-Jun. 2, 2014.
711 College Park, Maryland, USA: NOAA Coral Reef Watch. Data set accessed 2020-09-01
712 at ftp://ftp.star.nesdis.noaa.gov/pub/sod/mecb/crw/data/5km/v3.1/nc/v1.0/daily/dhw/.

713 NOAA Ocean Acidification Program. 2018. Ocean Acidification Research to Product
714 Development Workshop. US Dept Commer. NOAA Tech. Memo. **OAROAP-2**: 25.

715 Ogle, D., P. Wheeler, and A. Dinno. 2021. FSA: Fisheries Stock Analysis. R package version
716 0.8.32, <https://github.com/droglenc/FSA>.

717 Pacific Islands Fisheries Science Center. 2021. National Coral Reef Monitoring Program:
718 Benthic Cover from Annotated Benthic Images Collected During Photoquadrat Surveys
719 at Climate Stations across the Pacific Remote Island Areas since 2014,
720 <https://www.fisheries.noaa.gov/inport/item/36148>.

721 Pacific Islands Fisheries Science Center, C. R. E. P. 2017a. National Coral Reef Monitoring
722 Program: Stratified Random Surveys (StRS) of Reef Fish, including Benthic Estimate
723 Data at Jarvis and Wake from 2017-04-02 to 2017-04-23
724 (<https://www.ncei.noaa.gov/archive/accession/0163747>). NOAA Natl. Cent. Environ. Inf.
725 Dataset.

726 Pacific Islands Fisheries Science Center, C. R. E. P. 2017b. National Coral Reef Monitoring
727 Program: Stratified Random Surveys (StRS) of Reef Fish, including Benthic Estimate
728 Data of the Hawaiian Archipelago from 2016-07-13 to 2016-09-27
729 (<https://www.ncei.noaa.gov/archive/accession/0157590>). NOAA Natl. Cent. Environ. Inf.
730 Dataset.

731 Pacific Islands Fisheries Science Center, C. R. E. P. 2017c. National Coral Reef Monitoring
732 Program: Stratified Random Surveys (StRS) of Reef Fish, including Benthic Estimate
733 Data of the Mariana Archipelago from 2017-05-03 to 2017-06-20
734 (<https://www.ncei.noaa.gov/archive/accession/0166381>). NOAA Natl. Cent. Environ. Inf.
735 Dataset.

736 Pacific Islands Fisheries Science Center, E. S. D. 2019a. National Coral Reef Monitoring
737 Program: Stratified random surveys (StRS) of reef fish, including benthic estimate data
738 across the Pacific Remote Island Areas from 2018-06-08 to 2018-08-11

739 (<https://www.ncei.noaa.gov/archive/accession/0183544>). NOAA Natl. Cent. Environ. Inf.
740 Dataset.

741 Pacific Islands Fisheries Science Center, E. S. D. 2019b. National Coral Reef Monitoring
742 Program: Stratified random surveys (StRS) of reef fish, including benthic estimate data
743 across American Samoa from 2018-06-19 to 2018-07-18
744 (<https://www.ncei.noaa.gov/archive/accession/0183543>). NOAA Natl. Cent. Environ. Inf.
745 Dataset.

746 Perry, C. T., and L. Alvarez-Filip. 2019. Changing geo-ecological functions of coral reefs in the
747 Anthropocene. *Funct. Ecol.* **33**: 976–988. doi:10.1111/1365-2435.13247

748 Perry, C. T., L. Alvarez-Filip, N. A. J. Graham, and others. 2018a. Loss of coral reef growth
749 capacity to track future increases in sea level. *Nature* **558**: 396–400. doi:10.1038/s41586-
750 018-0194-z

751 Perry, C. T., I. Lange, and F. A. Januchowski-Hartley. 2018b. ReefBudget Indo Pacific: online
752 resource and methodology. Retrieved from <http://geography.exeter.ac.uk/reefbudget/>.

753 Perry, C. T., G. N. Murphy, N. A. J. J. Graham, S. K. Wilson, F. A. Januchowski-Hartley, and H.
754 K. East. 2015. Remote coral reefs can sustain high growth potential and may match future
755 sea-level trends. *Sci. Rep.* **5**: 18289. doi:10.1038/srep18289

756 Perry, C. T., G. N. Murphy, P. S. Kench, S. G. Smithers, E. N. Edinger, R. S. Steneck, and P. J.
757 Mumby. 2013. Caribbean-wide decline in carbonate production threatens coral reef
758 growth. *Nat. Commun.* **4**: 1402. doi:10.1038/ncomms2409

759 Pinheiro, J., D. Bates, S. DebRoy, /d Sarkar, and R Core Team. 2019. nlme: Linear and
760 Nonlinear Mixed Effects Models. R package verision 3.1-139. [https://CRAN.R-](https://CRAN.R-project.org/package=nlme)
761 [project.org/package=nlme](https://CRAN.R-project.org/package=nlme),.

762 Randall, C. J., and R. van Woesik. 2017. Some coral diseases track climate oscillations in the
763 Caribbean. *Sci. Rep.* **7**: 5719. doi:10.1038/s41598-017-05763-6

764 Reynolds, T., D. Burdick, P. Houk, L. Raymundo, and S. Johnson. 2014. Unprecedented coral
765 bleaching across the Marianas Archipelago. *Coral Reefs* **33**: 499–499.
766 doi:10.1007/s00338-014-1139-0

767 Skirving, W. J., S. F. Heron, B. L. Marsh, G. Liu, J. L. De La Cour, E. F. Geiger, and C. M.
768 Eakin. 2019. The relentless march of mass coral bleaching: a global perspective of
769 changing heat stress. *Coral Reefs* **38**: 547–557. doi:10.1007/s00338-019-01799-4

770 Skirving, W., B. Marsh, J. De La Cour, G. Liu, A. Harris, E. Maturi, E. Geiger, and C. M. Eakin.
771 2020. CoralTemp and the Coral Reef Watch Coral Bleaching Heat Stress Product Suite
772 Version 3.1. *Remote Sens.* **12**: 3856. doi:10.3390/rs12233856

773 Smith, S. V., and G. S. Key. 1975. Carbon Dioxide and Metabolism in Marine Environments.
774 *Limnol. Oceanogr.* **20**: 493–495. doi:10.4319/lo.1975.20.3.0493

775 Tribble, G. W., F. J. Sansone, and S. V. Smith. 1990. Stoichiometric Modeling of Carbon
776 Diagenesis Within a Coral-Reef Framework. *Geochim. Cosmochim. Acta* **54**: 2439–
777 2449.

778 Van Hooijdonk, R., J. Maynard, J. Tamelander, and others. 2016. Local-scale projections of coral
779 reef futures and implications of the Paris Agreement. *Sci. Rep.* **6**: 39666.
780 doi:10.1038/srep39666

781 Vargas-Ángel, B., B. Huntington, R. E. Brainard, R. Venegas, T. Oliver, H. Barkley, and A.
782 Cohen. 2019. El Niño-associated catastrophic coral mortality at Jarvis Island, central
783 Equatorial Pacific. *Coral Reefs* **38**: 731–741. doi:10.1007/s00338-019-01838-0

784 Venti, A., D. Kadko, A. J. Andersson, C. Langdon, and N. R. Bates. 2012. A multi-tracer model
785 approach to estimate reef water residence times. *Limnol. Oceanogr. Methods* **10**: 1078–
786 1095. doi:10.4319/lom.2012.10.1078

787 Williams, I. D., C. S. Couch, O. Beijbom, T. A. Oliver, B. Vargas-Angel, B. D. Schumacher, and
788 R. E. Brainard. 2019. Leveraging Automated Image Analysis Tools to Transform Our
789 Capacity to Assess Status and Trends of Coral Reefs. *Front. Mar. Sci.* **6**.
790 doi:10.3389/fmars.2019.00222

791 Woodhead, A. J., C. C. Hicks, A. V. Norström, G. J. Williams, and N. A. J. Graham. 2019. Coral
792 reef ecosystem services in the Anthropocene. *Funct. Ecol.* **33**: 1023–1034.
793 doi:10.1111/1365-2435.13331

794 Yates, K. K., D. G. Zawada, N. A. Smiley, and G. Tiling-Range. 2017. Divergence of seafloor
795 elevation and sea level rise in coral reef ecosystems. *Biogeosciences* **14**: 1739–1772.
796 doi:https://doi.org/10.5194/bg-14-1739-2017

797 Yeakel, K. L., A. J. Andersson, N. R. Bates, T. J. Noyes, A. Collins, and R. Garley. 2015. Shifts
798 in coral reef biogeochemistry and resulting acidification linked to offshore productivity.
799 *Proc. Natl. Acad. Sci.* **112**: 14512–14517. doi:10.1073/pnas.1507021112

800